COBEM 2023 27TH INTERNATIONAL CONGRESS OF MECHANICAL ENGENEERING

ABCM Brazilian Society of Mechanical Sciences and Engineering
27th ABCM International Congress of Mechanical Engineering
December 04-08, 2023, Florianópolis-SC, Brazil

COB-2023-0367
TORREFACTION OF URBAN FOREST WASTE: A PROCESS MODELING AND SIMULATION STUDY USING ASPEN PLUS SOFTWARE

Thiago da Silva Gonzales[1]
Mayara Gabi Moreira[2]
Giulia Lamas[3]
Pedro Paulo de Oliveira Rodrigues[4]
Thais Barbosa[5]
Matheus Neves Guedes[6]
Marcela Cardoso Rodrigues[7]
Simone Monteiro[8]
Edgar Amaral Silveira[9]
University of Brasília, Laboratory of Energy and Environment, Brasília, DF, 70910-900, Brazil
[1]thiagonzales@hotmail.com, [2]Mayaragabimoreira05@gmail.com, [3]giuliac.lamas@gmail.com, [4]pedropaulo9334@gmail.com, [5]barbosa31thais@gmail.com, [6]math_neves16@outlook.com, [7]marcelacrodrigues@gmail.com, [8]simonems@unb.br and [9]edgar.silveira@unb.br

Abstract. *Torrefaction is a promising thermochemical pretreatment method for biomass, which improves its energy properties as a solid biofuel. The torrefied product has coal-like properties and optimized characteristics for sustainable energy and heat generation, improving biomass properties like energy density, hydrophobicity, decomposition resistance, and storage performance. In this study, a biomass torrefaction model was developed to provide essential information for waste-to-energy solutions, specifically for future exergetic analysis. Experimental data from a blend of urban forest waste (UFW) from the forest ecosystem of Brasilia was used as input for simulations. The model, implemented in Aspen Plus® software, was validated under various torrefaction temperature scenarios (225-275°C), showing good agreement with reported experimental data (Absolute Deviation < 5%). The torrefaction module was successfully modeled using an RYield reactor, employing a two-step kinetic reaction model for biomass decomposition. Process consumed approximately 1549 kJ.kg^{-1} of biomass, with drying accounting for 70-88% of the total heat demand, depending on process conditions. The model demonstrated the ability to i) provide detailed distribution of products and by-products during the biomass torrefaction process and ii) predict important fuel properties such as proximate and elemental analyses. Additionally, the model allows the estimation of energy performance properties and overall energy consumption.*

Keywords: *Aspen Plus, sustainable energy, biomass charcoal, thermoconversion, tree trimmings*

1. INTRODUCTION

In recent years, studies on the utilization of biomass residues have gained momentum in the Brazilian energy industry (Lamas et al., 2022; Maria et al., 2023; Ribeiro et al., 2022). Moreover, these materials, due to their renewable nature and potential to replace fossil fuels, have become the subject of numerous academic studies aiming to find viable solutions for a more sustainable future (Evaristo et al., 2021; Fortes, 2022; Granado et al., 2021; Silveira et al., 2023). Lignocellulosic biomass, in its natural state, presents several inherent disadvantages, such as highly variable composition, low energy density, high moisture and oxygen content, and a hydrophilic nature. Typically, its composition consists of approximately 80% volatile materials and 20% fixed carbon on a dry basis. Therefore, to achieve higher energy efficiency and yield, it is necessary to overcome these challenges (Basu, 2018; W.-H. Chen et al., 2015; Sokhansanj et al., 2015).

Torrefaction emerges as a viable pretreatment technique applied to biomass. This thermochemical process is typically conducted in inert or partially oxidizing atmospheres between 200–300 °C (Basu, 2018; W. H. Chen and Kuo, 2011; Macedo et al., 2022; Silveira et al., 2023; Sokhansanj et al., 2015). The purpose of this thermal treatment is to reduce the volatile content, mainly related to hemicellulose degradation and the release of hydrogen and oxygen components, thus converting raw biomass into carbon-rich solid fuels. This process improves biomass properties such as energy density, hydrophobicity, decomposition resistance, and storage performance (Basu, 2018; Faria et al., 2021; Silveira et al., 2023; Sokhansanj et al., 2015; Xu et al., 2021).

Lignocellulosic biomass residues encompass wood, agro-industrial materials, and urban forest waste (UFW), which are characterized by rigid and fibrous structures and have low protein content and digestibility (Dai et al., 2019; Ghesti et al., 2022; Silveira et al., 2023). Afforestation in urban areas can directly influence the quality of life for the population by providing several benefits such as thermal comfort, shade, pollution reduction, and noise reduction (Silveira et al., 2023).

However, regular pruning is required for safety maintenance, which involves removing leaves, roots, trunks, dead branches, and diseased trees. As a result, one of the most common types of UFW waste is generated, which is usually available throughout the year and unfortunately often ends up in landfills (Bispo et al., 2021; Nowak et al., 2019; Silveira et al., 2023; Souza, 2014).

According to Brasilia's Solid Waste Management Plan, approximately 200 m³ of vegetable waste and an additional 100 m³ of large logs and firewood are collected daily (Governo do Distrito Federal, 2018). Previous studies have characterized the mixtures of various woody species found in urban forest waste (UFW) from Brasilia, the capital of Brazil, assessing their physical, chemical, and energy properties. These studies have focused on enhancing the thermal properties of UFW through torrefaction treatment and evaluating the resulting torrefied product. They have established linear correlations to predict properties such as kinetic performance, optimized mixtures, and torrefaction process conditions (Silveira et al., 2023).

This present study aims to conduct a comprehensive assessment of mass and energy balances of the UFW torrefaction process by Aspen Plus® V12.1 software. The data obtained in this work are fundamental to perform life cycle assessment and exergetic balances and, thus, to fully understanding the potential of tree pruning residues as a biofuel.

2. METHODOLOGY

2.1 Torrefaction kinetics modeling

For the present investigation, it is assumed that both untreated and torrefied biomass consist of solid materials containing carbon (C), hydrogen (H), oxygen (O), nitrogen (N), sulfur (S), and ash (A). The volatiles are mainly composed of acetic acid (CH_3COOH), water (H_2O), formic acid (HCOOH), methanol (CH_3OH), lactic acid (CH3-CH(OH)-COOH), furfural (C_4H_3OCHO), hydroxy acetone (CH_3COCH_2OH), carbon dioxide (CO_2), and carbon monoxide (CO) (Figure 1) (Bates and Ghoniem, 2012; Prins et al., 2006a, 2006b). A kinetic model must be adopted to determine the mass yields of torrefied biomass and the volatile materials released during the treatment. In this study, the two-step reaction model, originally proposed by Di Blasi and Lanzetta (1997), was adopted. Initially developed for hemicellulose degradation, the model comprises a competitive mechanism of first-order reactions divided into two steps (Figure 2) (Di Blasi and Lanzetta, 1997; Lanzetta and Di Blasi, 1998).

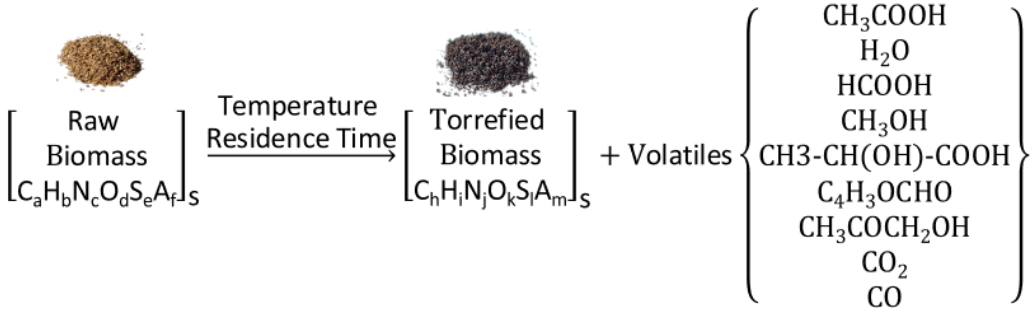

Figure 1. Raw biomass conversion. Adapted from (Bach et al., 2017a; Basu, 2018; Bates and Ghoniem, 2012).

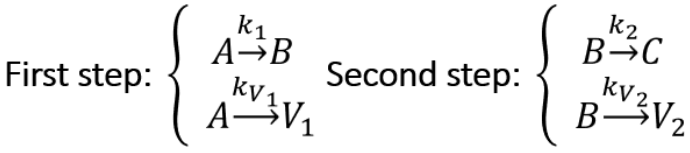

Figure 2. Diagram of the two-step reaction model.

This model is widely employed to describe the torrefaction kinetics of a large variety of biomasses, enabling the modeling of biomass decomposition into its pseudo-components (Bach et al., 2017a; Bates and Ghoniem, 2012; Haseli, 2018; Manouchehrinejad and Mani, 2019; Mukherjee et al., 2022; Onsree et al., 2020; Silveira et al., 2023). According to the proposed model, *A* represents the original biomass undergoing pretreatment, *B* is an intermediate solid product, *C* is the residual solid product. The volatile fraction released during the process is ascribed to V_1 and V_2. The terms k_1, k_{VI}, k_2 and k_{V2} denote the four Arrhenius kinetic parameters and can be determined by fitting the experimental thermogravimetric (TG) curves (mass loss) and numerical predicted data. Those set of reactions follows the first-order model (Bates and Ghoniem, 2012; Di Blasi and Lanzetta, 1997; Prins et al., 2006a, 2006b), originating Eqs. (1–5) by integration.

$$Y_A = e^{[-(k_1+k_{V_1})t]}, \tag{1}$$

$$Y_B = \frac{k_1}{(k_2+k_{V_2})-(k_1+k_{V_1})}\left[e^{[-(k_1+k_{V_1})t]} - e^{[-(k_2+k_{V_2})t]}\right], \tag{2}$$

$$Y_{V_1} = \frac{k_{V_1}}{(k_1+k_{V_1})}\left[1 - e^{[-(k_1+k_{V_1})t]}\right], \tag{3}$$

$$Y_C = \frac{k_1 k_2}{(k_2+k_{V_2})-(k_1+k_{V_1})}\left[\frac{e^{[-(k_2+k_{V_2})t]}}{(k_2+k_{V_2})} - \frac{e^{[-(k_1+k_{V_1})t]}}{(k_1+k_{V_1})}\right] + \frac{k_1 k_2}{(k_2+k_{V_2})(k_1+k_{V_1})}, \tag{4}$$

$$Y_{V_2} = \frac{k_1 k_{V_2}}{(k_2+k_{V_2})-(k_1+k_{V_1})}\left[\frac{e^{[-(k_2+k_{V_2})t]}}{(k_2+k_{V_2})} - \frac{e^{[-(k_1+k_{V_1})t]}}{(k_1+k_{V_1})}\right] + \frac{k_1 k_{V_2}}{(k_2+k_{V_2})(k_1+k_{V_1})}, \tag{5}$$

The Arrhenius equation (Eq. (6)) describes the relationship between pre-exponential factor (A_{O_i}), activation energy (E_{a_i}), universal gas constant, denoted as R = 8.314 J.K^{-1}mol^{-1}, and temperature T $[K]$. The kinetic parameters were determined in previous studies (Silveira et al., 2023).

$$k_i = A_{0_i} e^{\left(\frac{-Ea_i}{RT}\right)}, \tag{6}$$

At the end of the process, the total final composition of the mass fraction of the solids (Y_{TS}) is determined by the sum of masses Y_A, Y_B, and Y_C, while total final composition of the mass fraction of the volatiles (Y_{TV}) is composed of the sum of V_1 and V_2 (Haseli, 2018). Y_{TV} can be subdivided according to the proportion of each of the nine components present in V_1 and V_2. Bates and Ghoniem (2012) studied the modeling and evolution of volatile products from the torrefaction of willow, where the composition of the volatiles released during torrefaction was qualitatively and quantitatively analyzed. These values served as the basis for the composition of the volatiles of the present work. In V_1, highly oxygenated species such as water, carbon dioxide, and acetic acid are found, while V_2 is mainly composed of condensable volatiles such as lactic acid, methanol, acetic acid, water, formic acid, and hydroxy acetone (Bates and Ghoniem, 2012).

A previous study provided the linear correlation between torrefaction temperature and proximate properties (equations with R^2 of ~0.98) (Silveira et al., 2023). Those linear correlation were applied within the Aspen Plus® modeling to calculate the FC, VM and Ash of the torrefied solid product.

The energy performance of the torrefied product was assessed by applying the higher heating value (HHV), its enhancement factor (EF), the energy yield and the energy-mass-co-benefit-index (EMCI), which represent the difference between energy yields (EY) and mass yield (Y_{TS}). The HHV was determined according to the correlation by Channiwala and Parikh (Eq. (7)) (Channiwala and Parikh, 2002). The EY, EF and EMCI were obtained using Eqs. (8–10), respectively.

$$HHV = 0.3491C + 1.1783H + 0.1005S - 0.1034O - 0.0151N, \tag{7}$$

$$EY = EF.Y_{TS}, \tag{8}$$

$$EF = \frac{HHV_{torr}}{HHV_{raw}}, \tag{9}$$

$$EMCI = EY - Y_{TS}, \tag{10}$$

2.2 Process simulation

The proximate and ultimate composition of a blend of UFW composed of six different tree species from the Brasília ecosystem was used as input data for this work (Table 1) (Silveira et al., 2023). The simulation of the torrefaction process was performed using Aspen Plus® according to the proposed flowsheet (Figure 3 and Table 2). The following considerations were assumed:

- Assumed the process to be isothermal and at steady state;
- Disregarding the particle size effect and intra-particle heat and mass transfer;
- Peng-Robinson equation of state with the Boston-Mathias alpha function to described vapor-liquid equilibria;
- Biomass and biochar produced were considered non-conventional components, and their enthalpy and density were predicted by the General Coal Enthalpy (HCOALGEN) and the Coal Density Models (DCOALIGT) in Aspen Plus®, respectively.
- Air composition was assumed to be 79% nitrogen and 21% oxygen on a molar basis;
- Nitrogen was added to simulate an inert environment during torrefaction.

Table 1. Proximate and ultimate compositions used as input for simulation. Adapted from (Silveira et al., 2023).

Properties	**Raw Feedstock**
Moisture content	30.00
Proximate analysis (%)	
Fixed carbon (FC)	17.90
Volatile matter (MV)	77.61
Ash (A)	4.49
Ultimate analysis (%)	
Carbon (C)	44.91
Hydrogen (H)	7.25
Nitrogen (N)	0.64
Oxygen* (O)	42.71
H/C	1.92
O/C	0.71
Calorific Power (MJ·kg^{-1})	
HHV	19.47

*O = 100 – C – H – N – ash

Table 2. Streams and blocks description

	Descriptions
Stream	
AIR	T = 25 °C; P = 1.0 atm; Flow rate = 5 kg·h^{-1} (Aspen Technology, 2021; Onsree et al., 2020)
BIOMASS	T = 25 °C; P = 1.0 atm; Flow rate = 1 kg·h^{-1}
N2COLD	T = 25 °C; P = 1.0 atm; Flow rate = 1.2 mL·min^{-1} of N_2 for every 100 mg of material for torrefaction (Ibrahim et al., 2013)
Block	
HEATER1	HEATER; T = 150 and 180 °C; P = 1.0 atm;
DRYER1	RSTOIC; T = 110 °C; P = 1.0 atm;
SEPA1	FLASH2; T = 110 °C; P = 1.0 atm;
R1	RYIELD; T = 225 – 275 °C; P=1.0 atm; Residence Time = 30 and 60 Min.

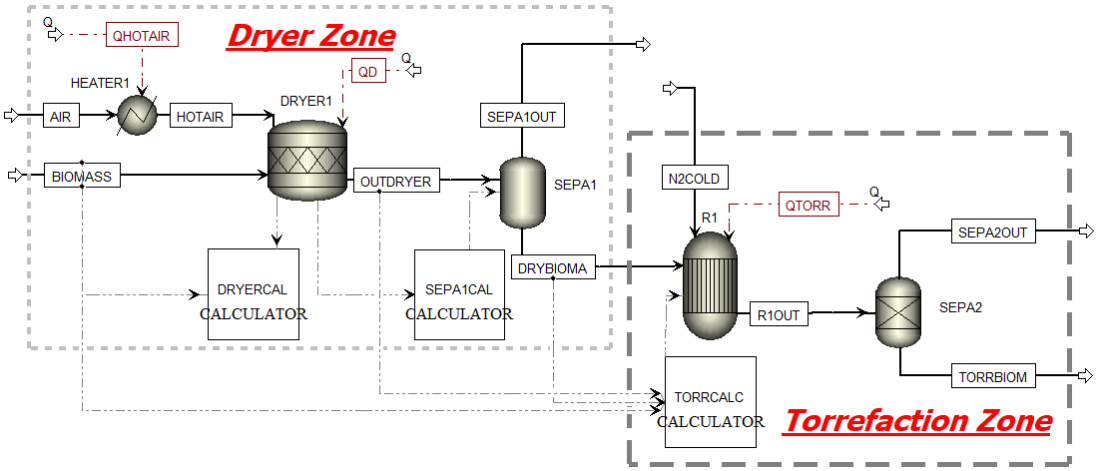

Figure 3. Torrefaction process workflow on Aspen-Plus.

The process was divided into two zones: the dryer and the torrefaction zones. The dryer zone consisted of a heater (HEATER block, named HEATER1), which provided the necessary energy to produce hot air used for drying the medium. The dryer itself was simulated by a stoichiometric reactor (RSTOIC block, named DRYER1), which provides the amount of water that is transferred to vapor phase, followed by a flash separation unit (FLASH2 block, named SEPA1) to separate the moist air (SEPA1OUT stream) from the dried biomass (DRYBIOMA stream). This configuration has been widely used in previous works (Aspen Technology, 2021; Awang et al., 2019; Mukherjee et al., 2022; Onsree et al., 2020). Additionally, a distinguished feature was added to the calculation block DRYERCAL to simulate the moisture removal step in the torrefaction process and SEPA1CALC to ensure the same temperature and pressure in the DRYER1 and

SEPA1 blocks. Furthermore, water recondensation in the dried biomass was prevented by setting the outlet temperature of DRYER1 at 110 °C (Bach et al., 2017a).

The torrefaction zone was simulated by combining the models of a yield reactor (RYield block, named R1), a calculator (referred to as TORRCALC), and a non-rigorous separation block (SEP, named SEPA2). The TORRCALC performed the integrated calculations of the yields for the formation of solid and volatile components according to Eqs. (1-6) with the kinetic parameters, defining the working conditions such as torrefaction temperature, residence time, and pressure. R1OUT was separated into two streams: the volatile material (SEPA2OUT) and the torrefied solid (TORRBIOM), using the non-rigorous separation block SEPA2. As a result, TORRBIOM consists solely of solid material, while SEPA2OUT consists entirely of gas.

For model validation, torrefaction was conducted assuming a complete absence of moisture, with a fixed residence time of 60 minutes at treatment temperatures of 225, 250, and 275 °C. These temperatures cover the three levels of torrefaction: mild (200–240 °C), moderate (240–260 °C), and severe (260–300 °C), as defined by (Basu, 2018). After validating the model and associated predicted properties, the energy balance was simulated to determine the amount of heat consumed throughout the entire process for the initial treatment of 1 $kg{\cdot}h^{-1}$ of wet biomass, considering different drying and torrefaction scenarios. Firstly, the drying medium, which is air, was heated in the range of 150 to 180 °C in the heat exchanger HEATER1. The final moisture content at the outlet of DRYER1 was adjusted between 0.5% and 10%. Subsequently, the torrefaction simulation was carried out at temperatures ranging from 240 to 275 °C for 30 and 60 minutes in the isothermal stage.

3. RESULTS AND DISCUSSIONS

3.1 Validation

The mass balance data obtained in the proposed model are presented in Table 3 and were compared with those found experimentally by Silveira et al. (2023) through absolute deviation (Figure (4a-d)). Regarding Table 3, the simulation showed low deviations for all studied parameters, including solid yield, proximate and ultimate composition, and energy indexes, which were suitable for the three analyzed temperatures. The highest deviations were observed at higher temperatures, which can be explained by the difficulty of conducting experiments under those conditions.

Table 3: Aspen Plus® simulation results for solid yield, ultimate and energy indexes and Absolute Deviation in Experimental data comparison (Silveira et al., 2023).

	Torrefaction treatment (°C)		
	225	**250**	**275**
Solid yield [a]			
Y_{TS}	94.21	87.10	75.27
Proximate [a]			
FC	20.37	24.40	31.10
MV	74.97	70.58	63.29
Ash	4.66	5.02	5.61
Ultimate [a]			
C	46.42	47.77	49.41
H	7.23	7.14	6.87
N	0.68	0.73	0.85
O	40.9	39.19	36.91
H/C	1.86	1.78	1.66
O/C	0.66	0.62	0.56
Energy indexes			
HHV[b]	20.16	20.69	21.16
EF	1.04	1.07	1.11
EY[a]	97.52	92.54	81.78
EMCI	3.31	5.44	6.51

In terms of carbon content (C%), the proposed torrefaction model tends to predict values lower than those found experimentally by Silveira et al. (2023). Conversely, for hydrogen (H) and oxygen (O), the experimental values are lower than those presented by the proposed model, and this difference increases with the severity of the torrefaction process. These results are directly related to the fixed proportion of volatiles used in Bates's work (Bates and Ghoniem, 2012). This fixed proportion of volatiles, which is commonly used to model torrefaction of various lignocellulosic biomasses in the literature (Chai et al., 2021), was obtained from the investigation of Willow biomass. However, it is important to

determine the specific volatile composition of the nine major components for each biomass to accurately predict the volatiles. This limitation will be further explored in future research.

The predictions of higher heating value (HHV), enhancement factor (EF), energy yield (EY), and energy-mass-co-benefit index (EMCI) correlated well with experimental data, showing an acceptable deviation as torrefaction severity increased.

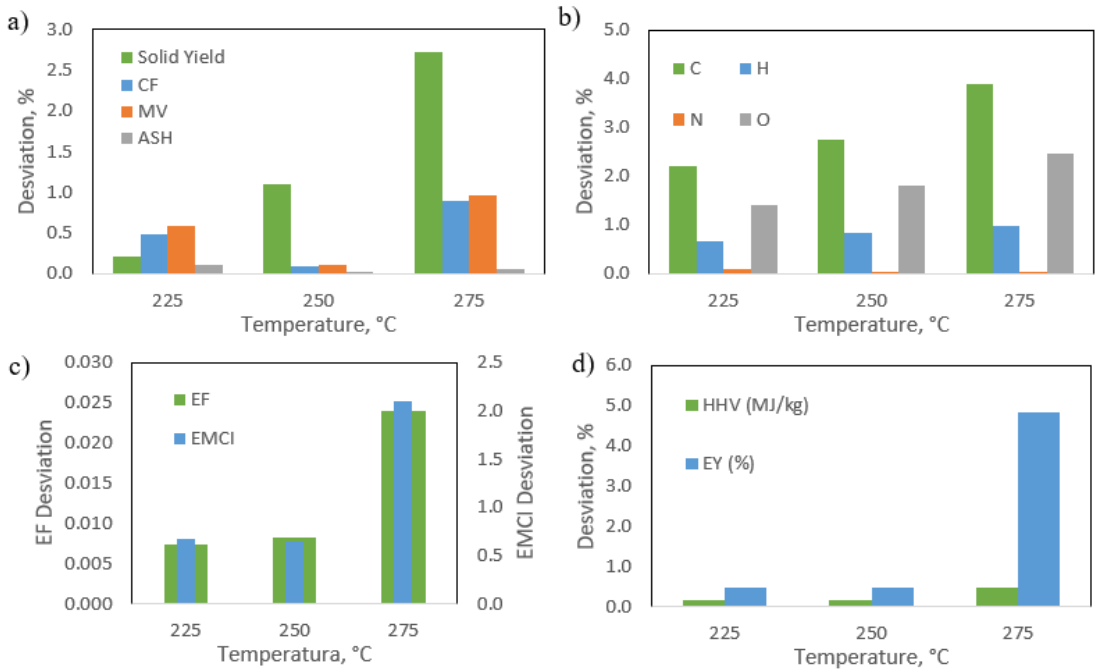

Figure 4. Simulation results versus Experimental data in Absolute Deviation (a) Solid Yield and Proximate Analysis (b) Ultimate Analysis. (c) EF and EMCI and (d) HHV and EY.

Regarding the literature on process simulation of torrefaction treatment, previous studies have simulated the torrefaction process of Norwegian Birch (Bach et al., 2017a), agricultural residues (Onsree et al., 2020), and coffee husk and spent coffee grounds (Mukherjee et al., 2022). For the torrefaction of Norwegian Birch (Bach et al., 2017a), the simulation resulted in higher values than the experimental results for solid yield, with a difference of up to 11.1% observed at 240 °C torrefaction. On the other hand, the investigation on the torrefaction of pellets produced from agricultural residues (Onsree et al., 2020) reported a difference of approximately 5% and 12% when comparing numerical and experimental data for torrefactions at 260 °C and 300 °C, respectively. Moreover, Mukherjee et al. (2022) successfully correlated data from their model with experimental data for the torrefaction of coffee husk and spent coffee grounds, but only at 200 °C. Above this temperature, the model yielded higher values than the experimental ones for both feedstocks.

The composition of elements found in the torrefaction gas is presented in Figure 5.

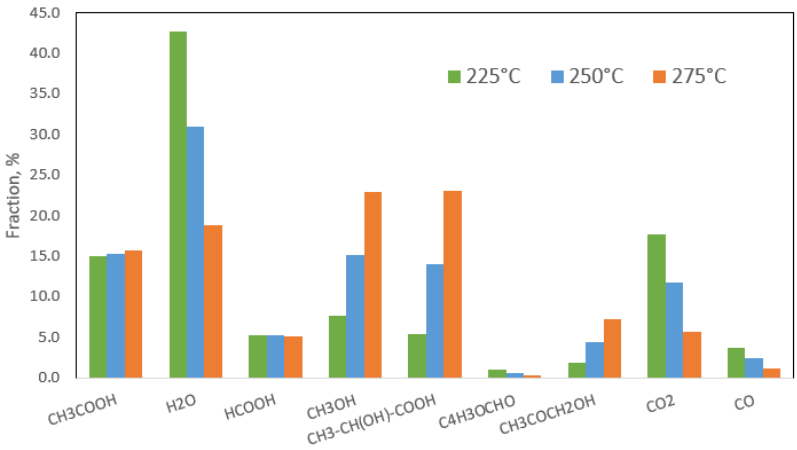

Figure 5. Volatile composition for torrefaction at 225, 250 and 275 °C.

Looking at the 225 °C treatment, a higher concentration of highly oxygenated species such as water, carbon dioxide, and acetic acid indicates a more significant formation of V_1, which accounts for 86.5% of Y_{TV}. As the torrefaction severity increases, there is a preference for the formation of condensable volatiles, including lactic acid, methanol, acetic acid, water, formic acid, and hydroxyacetone. These compounds indicate a higher presence of V_2, which corresponds to 72.4% of Y_{TV} in the composition of the torrefaction gas at 275 °C, consistent with the findings of (Chai et al., 2021).

3.2 Energy balance

The heat consumed in the drying stage is directly related to the specified final moisture. This heat consumption is referred to as $\dot{Q}_{dt}$ and is composed of the sum of $\dot{Q}_{hotair}$ and $\dot{Q}_{d}$. For example, complete moisture removal was achieved in the drying stage, requiring a heat consumption of 1318 kJ·h^{-1} (Figure (6a)). To reduce the initial moisture content to 5% and 10%, heat of 1235 kJ·h^{-1} and 1142 kJ·h^{-1}, respectively, was required.

Onsree et al. (2020) used 460 kJ kg^{-1} while drying 1.15 kg of pellets with 15% moisture, using 5 kg of fuel gas already at 150 °C. As their study did not include the heating of the drying medium, it is equivalent to only the step carried out in DRYER1, corresponding to the heat $\dot{Q}_{d}$ in the present work. As shown in Figure (6a), the required $\dot{Q}_{d}$ ranges between 352-682 kJ.kg^{-1} for 1 kg of UFW, which aligns with previous literature (Onsree et al., 2020). Moreover, a previous study investigated the drying of wood chips from 50% to 10% moisture content Manouchehrinejad and Mani (2019). In the drying of 34.5 Mg·h^{-1} wood chips, a heat consumption of 41,144 MJ·h^{-1} was reported, corresponding to 1192.60 kJ·kg^{-1}. Additionally, Bach et al. (2017b) used 363,240 kJ·h^{-1} for drying 200 kg of Norwegian birch from 50% to 10% moisture content. The air was employed as the drying medium, heated from 25 to 180 °C, with the biomass and moist air exiting the drying stage at 110 °C. Finally, the moist air was cooled to 50 °C, resulting in approximately 1816.2 kJ·kg^{-1} of heat consumption. In comparison, the present study, in terms of $\dot{Q}_{dt}$ (heat), exhibited an average heat consumption between 1142-1235 kJ·kg^{-1} per gram of material to dry biomass from 31% to a final moisture content of 10-5%.

Despite being in the same magnitude, differences in the amount of heat required in the drying stage for each biomass occur. These differences can be explained by variations in the biomass composition, which directly influence the specific heat of the raw material and consequently affect the heat flow consumed during the drying stage.

The Torrefaction Zone follows the Dryer zone (Figure 3). Table 3 and Figure (6b) display the results of the torrefaction treatments. The total heat consumption of the entire torrefaction process, $\dot{Q}_{total}$ (Table 4), for the biomass blend studied under the conditions described above was calculated by summing $\dot{Q}_{dt}$ and $\dot{Q}_{torr}$ (Figure (6a) and (6b)). These data show a slight increase in heat consumption as the moisture content of the biomass entering the torrefaction zone increases.

The model also reveals that drying is the most energy-consuming stage in the entire torrefaction process, consistent with (Basu, 2018). In the torrefaction of biomass with 5% moisture content, the heat used in drying accounts for 76-82% of the total heat demand in the process, while for 10% moisture content, it accounts for 70-75%, and in the absence of drying, it corresponds to 82-88%. Manouchehrinejad and Mani (2019) studied the torrefaction of pine wood chips with an initial moisture content of 50% at 270 °C and a residence time of 30 min. After drying, considering reducing the moisture content to 10%, the system consumed 80.06% of the evolved energy.

In the simulation of torrefaction of Norwegian birch branches (Bach et al., 2017a, 2017b), where the moisture content was reduced from 50% to 10%, the drying stage consumed 78-81% of the total energy consumed by the process in both studies.

Table 4. Total heat consumption of the entire torrefaction process.

Torrefaction(°C)	**$\dot{Q}_{total}$ (kJ.h^{-1})**					
	30 minutes			**60 minutes**		
	0% [a]	**5% [a]**	**10% [a]**	**0% [a]**	**5% [a]**	**10% [a]**
240	1493	1503	1513	1496	1506	1516
245	1502	1511	1522	1508	1517	1528
250	1511	1521	1532	1521	1531	1542
255	1521	1531	1543	1536	1546	1558
260	1533	1544	1555	1552	1562	1574
265	1546	1557	1569	1569	1580	1592
270	1561	1572	1585	1586	1598	1610
275	1576	1588	1601	1605	1616	1630

[a] moisture content after the drying zone.

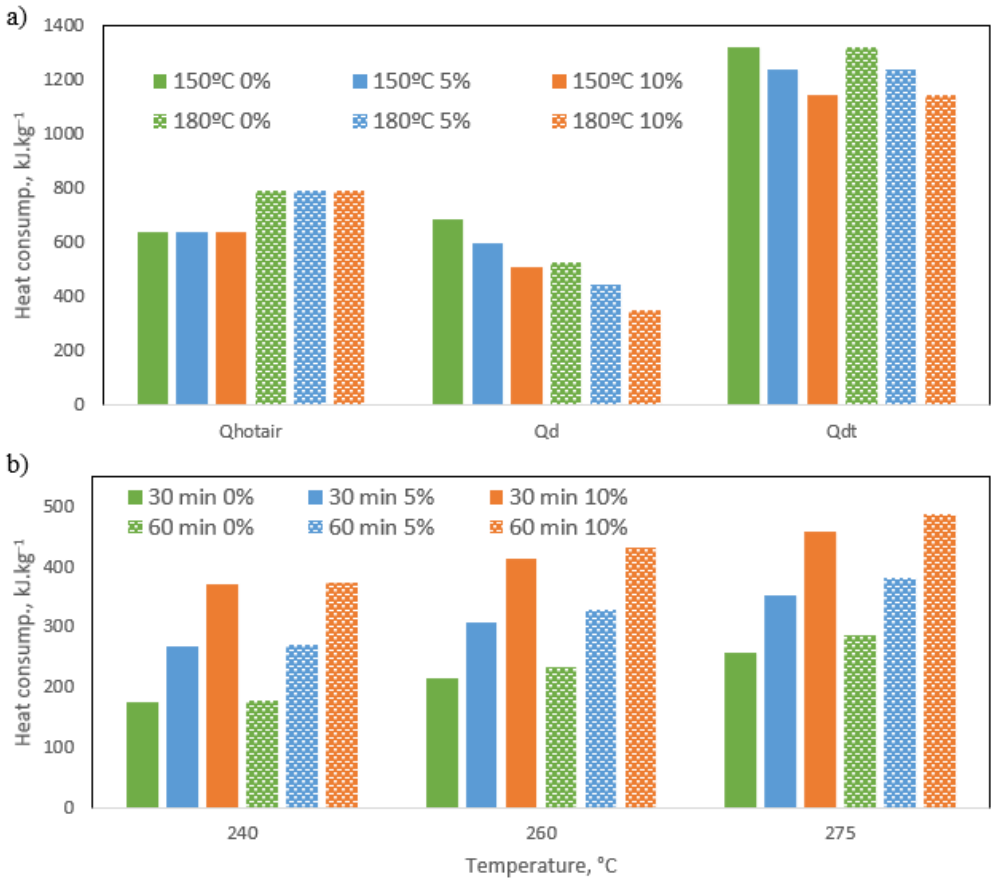

Figure 6. (a) Dryer heat consumption considering 150 and 180 °C drying temperatures and 0, 5 and 10% final moisture content. (b) Torrefaction heat consumption ($\dot{Q}_{torr}$) considering 30 and 60 min treatment and 240-275 °C temperatures.

Upon observing Table 4, along with Figures Figure (6a) and (6b), it becomes evident that, based on the proposed model, the assumed conditions, and for an initial flow rate of 1 kg.h^{-1} of wet biomass, the data show a monotonic trend behavior. The energy consumption required for the torrefaction treatment of the biomass falls within the range of 1493-1630 kJ.h^{-1}. This finding offers valuable insights and information for future endeavors, such as scaling up torrefaction plants and developing relevant policies. Additionally, further investigations encompassing exergy balances, coupled with environmental considerations (such as life cycle assessment (Deutsch et al., 2022; Silveira et al., 2017)) and economic factors, will be conducted. These efforts will enable a comprehensive analysis of the exergoeconomic and exergoenvironmental aspects of scaling up torrefaction plants in urban districts.

4. CONCLUSION

A torrefaction model was developed using Aspen Plus® V12.1 software. The model was validated against experimental data and compared with other models reported in the literature. It can predict the distribution of torrefied biomass and by-products, as well as the heat required for the torrefaction process. The simulation results demonstrate good agreement with experimental data available in the literature. Increasing the torrefaction temperature leads to a reduction in mass yields and an increase in the higher heating value (HHV) of the torrefied biomass. The carbon, oxygen, and hydrogen contents are consistent with experimental data; however, there is room for further improvement in prediction accuracy. The model also reveals that torrefaction pre-treatment consumes 1493 to 1630 kJ.h^{-1} for an initial flow rate of 1 kg.h^{-1} of wet biomass, and drying accounts for approximately 70 to 88% of the total heat demand, depending on the torrefaction conditions.

5. ACKNOWLEDGEMENTS

The research presented was supported by the Brazilian National Council for Scientific and Technological Development (CNPq), Coordenação de Aperfeiçoamento de Pessoal de Nível Superior - Brasil (CAPES) - Finance Code 001, Brazilian Forest Products Laboratory, DPI/UnB, DPG/UnB and Federal District Research Foundation (FAPDF – Project 81/2021, 3/2021).

6. REFERENCES

Aspen Technology. (2021). *Aspen Plus Help* (I. Aspen Technology (ed.); V12.1). Aspen Technology, Inc. https://web.ist.utl.pt/ist11038/acad/Aspen/AspUserGuide10.pdf

Awang, A. H., Abdulrazik, A., Nafsun, A. I., Halim, A., Razik, A. (2019). Modelling and Optimization of Torrefied Pellet Fuel Production. *Pertanika J. Sci. & Technol*, *27*(4), 2139–2152.

Bach, Q. V., Skreiberg, Ø., Lee, C. J. (2017a). Process modeling and optimization for torrefaction of forest residues. *Energy*, *138*, 348–354. https://doi.org/10.1016/j.energy.2017.07.040

Bach, Q. V., Skreiberg, Ø., Lee, C. J. (2017b). Process modeling for torrefaction of birch branches. *Energy Procedia*, *142*, 395–400. https://doi.org/10.1016/J.EGYPRO.2017.12.062

Basu, P. (2018). Biomass Gasification, Pyrolysis and Torrefaction: Practical Design and Theory. In *Biomass Gasification Design Handbook* (3rd ed.). Elsevier Inc. https://doi.org/https://doi.org/10.1016/B978-0-12-812992-0.00001-7

Bates, R. B., Ghoniem, A. F. (2012). Biomass torrefaction: Modeling of volatile and solid product evolution kinetics. *Bioresource Technology*, *124*, 460–469. https://doi.org/10.1016/j.biortech.2012.07.018

Bispo, L. F. P., Nolasco, A. M., Souza, E. C. de, Klingenberg, D., Dias Júnior, A. F. (2021). Valorizing urban forestry waste through the manufacture of toys. *Waste Management*, *126*, 351–359. https://doi.org/10.1016/J.WASMAN.2021.03.028

Chai, M., Xie, L., Yu, X., Zhang, X., Yang, Y., Rahman, M. M., Blanco, P. H., Liu, R., Bridgwater, A. V., Cai, J. (2021). Poplar wood torrefaction: Kinetics, thermochemistry and implications. *Renewable and Sustainable Energy Reviews*, *143*, 110962. https://doi.org/10.1016/J.RSER.2021.110962

Channiwala, S. A., Parikh, P. P. (2002). A unified correlation for estimating HHV of solid, liquid and gaseous fuels. *Fuel*, *81*(8), 1051–1063. https://doi.org/10.1016/S0016-2361(01)00131-4

Chen, W.-H., Peng, J., Bi, X. T. (2015). A state-of-the-art review of biomass torrefaction, densification and applications. *Renewable and Sustainable Energy Reviews*, *44*, 847–866. https://doi.org/10.1016/j.rser.2014.12.039

Chen, W. H., Kuo, P. C. (2011). Torrefaction and co-torrefaction characterization of hemicellulose, cellulose and lignin as well as torrefaction of some basic constituents in biomass. *Energy*, *36*(2), 803–811. https://doi.org/10.1016/J.ENERGY.2010.12.036

Dai, L., Wang, Y., Liu, Y., Ruan, R., He, C., Yu, Z., Jiang, L., Zeng, Z., Tian, X. (2019). Integrated process of lignocellulosic biomass torrefaction and pyrolysis for upgrading bio-oil production: A state-of-the-art review. *Renewable and Sustainable Energy Reviews*, *107*, 20–36. https://doi.org/10.1016/J.RSER.2019.02.015

Deutsch, L., Lamas, G. C., Pereira, T. S., Silveira, E. A., Caldeira-Pires, A. (2022). Life cycle and risk assessment of vinasse storage dams: A Brazilian sugar-energy refinery analysis. *Sustainable Futures*, *4*, 100083. https://doi.org/10.1016/J.SFTR.2022.100083

Di Blasi, C., Lanzetta, M. (1997). Intrinsic kinetics of isothermal xylan degradation in inert atmosphere. *Journal of Analytical and Applied Pyrolysis*, *40–41*, 287–303. https://doi.org/10.1016/S0165-2370(97)00028-4

Evaristo, R. B. W., Ferreira, R., Petrocchi Rodrigues, J., Sabino Rodrigues, J., Ghesti, G. F., Silveira, E. A., Costa, M. (2021). Multiparameter-analysis of CO2/Steam-enhanced gasification and pyrolysis for syngas and biochar production from low-cost feedstock. *Energy Conversion and Management: X*, *12*, 100138. https://doi.org/10.1016/J.ECMX.2021.100138

Faria, B. de F. H. de, Charline, L., Jeremy, V., Patrick, R., Oliveira Carneiro Angélica, D. C., Armando, C. P., Kévin, C. (2021). Emulation of field storage conditions for assessment of energy properties of torrefied sugarcane bagasses. *Biomass and Bioenergy*, *145*, 105938. https://doi.org/10.1016/j.biombioe.2020.105938

Fortes, M. M. (2022). Recuperação Energética de Resíduos Agroflorestais por meio de Peletização e Torrefação [Tese de doutorado em Ciências Florestais, Universidade de Brasília]. In *Departamento de Engenharia Florestal*. http://www.pgea.unb.br/~lasp/research/DEFESA_VALERIO_AYMORE_MARTINS_DM-500_2012.pdf

Ghesti, G. F., Silveira, E. A., Guimarães, M. G., Evaristo, R. B. W., Costa, M. (2022). Towards a sustainable waste-to-energy pathway to pequi biomass residues: Biochar, syngas, and biodiesel analysis. *Waste Management*, *143*, 144–156. https://doi.org/10.1016/J.WASMAN.2022.02.022

Governo do Distrito Federal. (2018). PDGIRS – Plano Distrital De Gestão Integrada De Resíduos Sólidos. In *Governo do Distrito Federal* (Vol. 3). Governo do Distrito Federal. http://www.sinesp.df.gov.br/wp-conteudo/uploads/2018/03/PDGIRS.pdf

Granado, M., Machado, G., Padilla, E., Yamaji, F. (2021, July). Torrefação do Resíduo da Mandioca para Fins Energéticos. *Revista Virtual de Química*, *13*. https://doi.org/10.21577/1984-6835.20210095

Haseli, Y. (2018). Process Modeling of a Biomass Torrefaction Plant. *Energy and Fuels*, *32*(4), 5611–5622. https://doi.org/10.1021/acs.energyfuels.7b03956

Ibrahim, R. H. H., Darvell, L. I., Jones, J. M., Williams, A. (2013). Physicochemical characterisation of torrefied biomass. *Journal of Analytical and Applied Pyrolysis*, *103*, 21–30. https://doi.org/10.1016/J.JAAP.2012.10.004

Lamas, G. C., Costa, F. C., Santanna, M. S., Chaves, B. S., Galvão, L. G. O., Macedo, L. A., Caldeira-Pires, A., Silveira, E. A. (2022). Steam-Enhanced Gasification of a Hybrid Blend Composed of Municipal Solid Waste and Torrefied Biomass. *European Biomass Conference and Exhibition Proceedings*, 205–213.

https://doi.org/10.5071/30THEUBCE2022-1CV.2.2

Lanzetta, M., Di Blasi, C. (1998). Pyrolysis kinetics of wheat and corn straw. *Journal of Analytical and Applied Pyrolysis*, *44*(2), 181–192. https://doi.org/10.1016/S0165-2370(97)00079-X

Macedo, L. A., Silveira, E. A., Rousset, P., Valette, J., Commandré, J. M. (2022). Synergistic effect of biomass potassium content and oxidative atmosphere: Impact on torrefaction severity and released condensables. *Energy*, *254*, 124472. https://doi.org/10.1016/J.ENERGY.2022.124472

Manouchehrinejad, M., Mani, S. (2019). Process simulation of an integrated biomass torrefaction and pelletization (iBTP) plant to produce solid biofuels. *Energy Conversion and Management: X*, *1*(January). https://doi.org/10.1016/j.ecmx.2019.100008

Maria, Í., Mendes, L., Socorro, M., Fialho, B., Leão, R. M., Silveira, E. A., Maria Da Luz, S. (2023). Processing Biodegradable Blends of Hemicellulose with Polyhydroxybutyrate and Poly (Lactic Acid). *Materials Research*, *26*, e20220390. https://doi.org/10.1590/1980-5373-MR-2022-0390

Mukherjee, A., Okolie, J. A., Niu, C., Dalai, A. K. (2022). Experimental and Modeling Studies of Torrefaction of Spent Coffee Grounds and Coffee Husk: Effects on Surface Chemistry and Carbon Dioxide Capture Performance. *ACS Omega*, *7*(1), 638–653. https://doi.org/10.1021/acsomega.1c05270

Nowak, D. J., Greenfield, E. J., Ash, R. M. (2019). Annual biomass loss and potential value of urban tree waste in the United States. *Urban Forestry & Urban Greening*, *46*, 126469. https://doi.org/https://doi.org/10.1016/j.ufug.2019.126469

Onsree, T., Jaroenkhasemmeesuk, C., Tippayawong, N. (2020). Techno-economic assessment of a biomass torrefaction plant for pelletized agro-residues with flue gas as a main heat source. *Energy Reports*, *6*(December), 92–96. https://doi.org/10.1016/j.egyr.2020.10.043

Prins, M. J., Ptasinski, K. J., Janssen, F. J. J. G. (2006a). Torrefaction of wood: Part 1. Weight loss kinetics. *Journal of Analytical and Applied Pyrolysis*, *77*(1), 28–34. https://doi.org/10.1016/J.JAAP.2006.01.002

Prins, M. J., Ptasinski, K. J., Janssen, F. J. J. G. (2006b). Torrefaction of wood: Part 2. Analysis of products. *Journal of Analytical and Applied Pyrolysis*, *77*(1), 35–40. https://doi.org/10.1016/J.JAAP.2006.01.001

Ribeiro, Y. H. M., Cruz Lamas, G., Castilho Faria Mendes, R., Simões Santanna, M., Caldeira-Pires, A., Amaral Silveira, E. (2022). Energy Recovery from Municipal Solid Waste Combustion and Agropastoral Bio-digestion: Analysis of the Technical Feasibility in Brazil'Capital. *European Biomass Conference and Exhibition Proceedings*, 228–234. https://doi.org/10.5071/30THEUBCE2022-1CV.2.7

Silveira, E. A., Caldeira-Pires, A., Luz, S. M., Silveira, C. M. (2017). Mass and energy allocation method analysis for an oil refinery characterization using multi-scale modeling. *International Journal of Life Cycle Assessment*, *22*(11), 1815–1822. https://doi.org/10.1007/S11367-017-1369-9

Silveira, E. A., Santanna, M. S., Barbosa Souto, N. P., Lamas, G. C., Galvão, L. G. O., Luz, S. M., and Caldeira-Pires, A. (2023). Urban lignocellulosic waste as biofuel: thermal improvement and torrefaction kinetics. *Journal of Thermal Analysis and Calorimetry*. https://doi.org/10.1007/s10973-022-11515-0

Sokhansanj, S., Melin, S., Madrali, S., Cremers, M., Koppejan, J., Middelkamp, J., Witkamp, J. (2015). *Status overview of torrefaction technologies. A review of the commercialisation status of biomass torrefaction* (Task 32). IEA Bioenergy. https://www.ieabioenergy.com/blog/publications/status-overview-of-torrefaction-technologies-a-review-of-the-commercialisation-status-of-biomass-torrefaction/

Souza, M. M. de. (2014). *Propriedades de briquetes e pellets produzidos com resíduos sólidos urbanos* [Tese para obtenção do título de Doctor Scientiae em Ciências Florestais]. Universidade Federal de Viçosa.

Xu, J., Huang, M., Hu, Z., Zhang, W., Li, Y., Yang, Y., Zhou, Y., Zhou, S., Ma, Z. (2021). Prediction and modeling of the basic properties of biomass after torrefaction pretreatment. *Journal of Analytical and Applied Pyrolysis*, *159*, 105287. https://doi.org/10.1016/J.JAAP.2021.105287

7. RESPONSIBILITY NOTICE

The authors are the only responsible for the printed material included in this paper.